Fu *et al. Int J Concr Struct Mater* (2022) 16:31
https://doi.org/10.1186/s40069-022-00524-w

International Journal of Concrete Structures and Materials

RESEARCH Open Access

Flexural Behavior and Prediction Model of Basalt Fiber/Polypropylene Fiber-Reinforced Concrete

Qiang Fu[1,2*], Zhaorui Zhang[1], Wenrui Xu[1], Xu Zhao[1], Lu Zhang[1], Yan Wang[3*] and Ditao Niu[1,2]

Abstract

The flexural behavior of basalt fiber (BF)/polypropylene fiber (PF)-reinforced concrete (BPRC) was investigated. When the content of BF and PF is 0.1%, the addition of fibers increases the compressive strength of concrete. A BF content of 0.1% has the most obvious effect on improving the compressive strength, but a hybrid fiber content of 0.2% exhibits a negative effect on the compressive strength. The addition of BF and PF can increase the flexural strength and the expansion tortuosity of the fracture cracks, thus enhancing the ductility of concrete. The hybrid fibers with content of 0.1% are most beneficial to increase the flexural strength. However, the ductility of concrete and the tortuosity of fracture crack decrease with the matrix strength, and the improvement proportion of fibers on the flexural strength also decreases. When the BF and PF are mixed, compared to the case of single fiber added, there is no significant change in the damage of BF, whereas the damage of PF is more severe. The flexural toughness index FT_δ effectively characterizes the change in the flexural toughness of BPRC. The hybrid fiber contents of 0.1% and 0.2% exhibit the most significant improving effect on *FT-l*/600 and *FT-l*/150, respectively. Considering the influence of fibers on the compressive strength, flexural strength and flexural toughness of concrete, a hybrid content of 0.1% is the optimal choice of fiber content. A prediction model for flexural strength of BPRC is proposed based on the composite material theory.

Keywords: fiber, matrix strength, flexural toughness, prediction model

1 Introduction

With the development of society, concrete is more and more used in the construction of various engineering structures. However, because of high brittleness, ordinary concrete has low flexural properties and fracture toughness, and is easy to crack, which significantly affects its durability. Currently, strengthening concrete with fiber-reinforced polymer or adding fibers in concrete can effectively reduce the brittleness of concrete and improve its toughness (Domenico et al., 2020; Walton et al., 1975). Among them, adding fibers is the most widely used toughening method of concrete around the world. (Banthia et al., 2007; Dong et al., 2019; Yoo et al., 2013; Zhong et al., 2020). As the cracking of concrete is a multi-scale process from the material scale to the structural scale, the flexural properties and fracture toughness of concrete can be effectively improved by adding various fibers and playing their roles of crack limiting in different scales (Dong et al., 2008; Li et al., 2018a; Uygunoglu et al., 2008). The mixing of steel fiber and polypropylene fiber (PF) is the most effective and recognized mixing mode that improves the fracture toughness of concrete (Bhutta et al., 2017; Li et al., 2018a; Mastali et al., 2018; Sukontasukkul et al., 2018; Wang et al., 2012; Yap et al., 2014; Zhong et al., 2020). The steel fiber with high strength effectively enhances the cracking strength of concrete, and PF with low strength increases the ductility of

*Correspondence: fuqiangcsu@163.com; 179442766@qq.com
[1] School of Civil Engineering, Xi'an University of Architecture and Technology, Xi'an 710055, People's Republic of China
[3] College of Materials Science and Engineering, Xi'an University of Architecture and Technology, Xi'an 710055, People's Republic of China
Full list of author information is available at the end of the article
Journal information: ISSN 1976-0485 / eISSN 2234-1315

concrete. The cooperation of steel fiber and PF improves the fracture toughness of concrete.

The corrosion of steel bars due to chloride ion action is the primary cause of the property degeneration of structures in marine environments. Therefore, the easy corrosion of steel fibers can accelerate the property degeneration of marine engineering structures made of hybrid steel fiber/polypropylene fiber-reinforced concrete (Marcos-Meson et al., 2018). Basalt fiber (BF) is an environment-friendly fiber that has increasingly been used in concrete materials in recent years. BF is made of basalt rock that is melted at high temperatures and drawn into wires, and the production process consumes a small amount of energy. BF has good mechanical properties and strong acid and alkali corrosion resistance. In addition, the compatibility between BF and cement-based materials is good (Dilbas et al., 2020; Ralegaonkar et al., 2018; Rybin et al., 2013; Smarzewski, 2020; Sun et al., 2019; Wang et al., 2019). Therefore, through replacing steel fibers with BF, the hybrid BF/PF-reinforced concrete (BPRC) can be used to enhance the fracture toughness and durability of concrete in marine environments.

Existing research on BPRC is primarily focused on the impact resistance and basic mechanical properties (compressive, splitting tensile, and flexural properties). Fu et al. (2018) and Zhang et al. (2019) demonstrated that mixed BF and PF can effectively improve the impact resistance of concrete. BF is helpful to enhance the impact strength, but PF is helpful to increase the impact toughness of concrete. Wang et al. (2019) studied hybrid BF/PF-reinforced high-performance concrete, and revealed that when BF content was 0.15% and PF content was 0.033%, the compressive, flexural, and splitting tensile strength of the high-performance concrete increased by 14.1%, 22.8%, and 48.6%, respectively. Shi et al., (2020) obtained similar results to those obtained by Wang et al. (2019) by studying the mechanical properties of hybrid BF/macro-PF-reinforced concrete. However, they recommended a significantly different optimal fiber content. Smarzewski (2019) systematically investigated the influence of single BF, PF, and hybrid BF and PF on the compressive, splitting tensile, and flexural strength of high-performance concrete. The addition of single or hybrid fibers reduced the compressive strength, and improved the splitting tensile strength and flexural strength of concrete. The hybrid fibers had a more obvious enhancement effect on the flexural strength and fracture energy of concrete than the single fiber.

At present, only a few research works on the flexural properties of BPRC primarily focus on the influence of hybrid BF and PF on the fracture properties of high-performance concrete, and the influence mechanism of BF and PF on the flexural properties of concrete has not been clarified. In addition, the prediction model for the flexural strength of BPRC has also not been established. For ordinary concrete, the difference between its matrix properties and the ones of high-performance concrete will inevitably lead to different effects of BF and PF on the flexural properties. However, the comprehensive study on the influence of hybrid BF and PF on the flexural properties of ordinary concrete has not been reported. In this study, the flexural properties of ordinary concrete with different matrix strengths and different adding mode of BF and PF are investigated. The flexural load–deflection curve of BPRC is obtained. The variations in the flexural strength, fracture morphology of BPRC, and failure morphology of fibers with matrix strengths are systematically analyzed. The change rule of the flexural toughness of BPRC is discussed, and the effective evaluation index of flexural toughness is determined. Finally, a prediction model for flexural strength of BPRC is established based on composite material theory. The obtained results have a good reference for the design of BPRC according to the specific flexural performance.

2 Materials and Experimental Framework

2.1 Raw Materials and Sample Preparation

The binding materials used herein are Portland cement (P.O 42.5R, C), silica fume (SF), fly ash (FA), and slag powder (SP), and their parameters are listed in Niu et al. (2020). The river sand was used as fine aggregate (S), and has a maximum particle size of 4.75 mm and a fineness modulus of 2.8. The coarse aggregate (CA) was mechanically crushed limestone, with a particle size of 5–20 mm and an apparent density of 2.7 g/cm^3. Additionally, the drinkable tap water (W) and polycarboxylate superplasticizer (PBS) with a water reduction rate of 30% were used to mix the materials. The fiber reinforcement materials include BF and PF as shown in Fig. 1, and their parameters are also listed in Niu et al., (2020).

The BPRC mixture compositions designed herein are displayed in Table 1, wherein OC represents the reference concrete, and BRC, PRC, and BPRC represent the

Fig. 1 Morphologies of **a** BF and **b** PF.

Table 1 BPRC mixture proportions (kg/m^3).

Mixture	BF	PF	C	W	SF	FA	SP	S	CA	PBS	Slump (mm)
OC-30	0	0	234.2	161	22	73.2	36.6	683	1162.9	3.66	185
BRC-30-0.1	2.56	0									86
PRC-30-0.1	0	0.91									68
BPRC-30-0.1	1.28	0.455									132
BPRC-30-0.2	2.56	0.91									90
OC-40	0	0	241.6	150.5	15.8	79.2	59.4	683.4	1163.6	3.96	186
BRC-40-0.1	2.56	0									123
PRC-40-0.1	0	0.91									165
BPRC-40-0.1	1.28	0.455									158
BPRC-40-0.2	2.56	0.91									97
OC-50	0	0	333.1	140	29	48.3	72.4	774.1	1026.1	4.83	115
BRC-50-0.1	2.56	0									54
PRC-50-0.1	0	0.91									91
BPRC-50-0.1	1.28	0.455									102
BPRC-50-0.2	2.56	0.91									35

mixtures containing single BF, single PF, and hybrid BF and PF, respectively. When BF and PF are mixed, they are added into the mixture with the same content. The first number after the letter indicates the strength grade of matrix (e.g., C30, C40, and C50), and the second number represents the fiber volume content (%).

As shown in Fig. 2, to prepare the BPRC mixture, first, CA and S were mixed for 30 s. Then, C, SF, FA and SP were added into the mixture, and stirred for 2 min. Next, PF and BF were added in turn, and stirred for 2 min and 3 min, respectively. Finally, the hybrid PBS and W were added and stirred for 2 min. Immediately after mixing, the slump of the BPRC mixture was tested using a slump cylinder (GB/T50080-2016, 2016), and the test results are listed in Table 1. Then, the BPRC mixture was poured into 100 mm × 100 mm × 100 mm cubic molds and 100 mm × 100 mm × 400 mm prismatic molds, and compacted on a vibrating table. After 24 h of curing in a room with temperature of 20 ± 2 °C, relative humidity of > 95%, the specimens were demolded, and continuously cured to the age of 28 days before the relevant mechanical properties were tested.

2.2 Testing Methods

2.2.1 Compressive Strength Test

The compressive strength of BPRC specimens was tested using an electro-hydraulic pressure servo testing machine. The specimen with a size of 100 mm × 100 mm × 100 mm was tested at the loading rate of 0.5 MPa/s (GB/T50081-2002, 2002). Before the formal loading process, the two loading surfaces of the specimen and the surfaces of the upper and lower pressure plates were coated with a thin layer of lubricating oil to effectively reduce the friction between the specimen and the pressure plates. Five specimens were tested for each mixture proportion of BPRC, and the average value of the test results was taken as the final experimental result. A total of 75 specimens were used to test the compressive strength of BPRC.

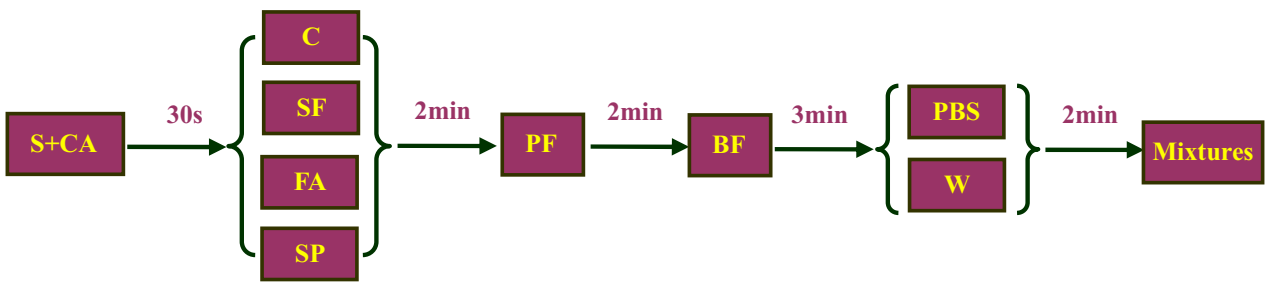

Fig. 2 Schematic of BPRC mixing process.

2.2.2 Flexural Test

The flexural properties of BPRC specimen were tested using a DNS300 electronic universal testing machine. The specimen with a size of 100 mm × 100 mm × 400 mm was tested at the loading mode of four-point bending loading (GB/T50081-2002, 2002). The loading diagram is shown in Fig. 3. The bottom surface of the test specimen was supported by two steel cylinders. The distance between the axes of the two steel cylinders was 300 mm, and the distance between the axes of the two steel cylinders and the ends of the specimen were 50 mm. The distance between the axes of the two loaded steel cylinders on the top surface of the specimen was 100 mm. The distance between the axes of the two steel cylinders on the top surface and the ends of the specimen were 150 mm. The rate of flexural loading was 0.1 mm/min. The deflection of the specimen was measured using two linear variable displacement transducers (LVDTs) that were fixed on the side of the specimen. The average value of the deformation measured by the two LVDTs was recorded as the final result of the bending deflection of the BPRC specimens. The two LVDTs were fixed in the middle of the specimen using a support frame that was mounted on the specimen. The cross bar of the supporting frame could rotate freely, which allowed the two LVDTs to measure the net deflection of the midspan of the BPRC specimen (Banthia et al., 2007; He et al., 2020; Wu et al., 2020). Under each condition, the number of repeated specimens and the determination method of the final flexural experimental results were consistent with those for the compressive strength test. A total of 75 specimens were used to test the flexural properties of BPRC.

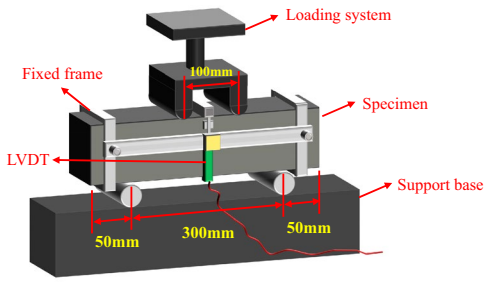

Fig. 3 Loading diagram of four-point bending test.

3 Evaluation Index of Flexural Toughness of BPRC

According to the load–deflection curves of BPRC, the post-crack strength (*PCS*), equivalent flexural strengths (f_{eq1}, f_{eq2}), and flexural toughness factor (FT_δ) were calculated to characterize the flexural toughness of BPRC (Banthia et al., 2007, 2014; CECS13, 2009).

In this study, the *PCS* of BPRC can be calculated as (Banthia et al., 2007):

$$\mathrm{PCS} = \frac{T_{\mathrm{post}} l}{(\delta - \delta_{\mathrm{p}}) b h^2}, \tag{1}$$

where l, b, and h represent the span, width, and height of the BPRC specimen, respectively; δ is the set deflection, where δ=l/600 and l/150 herein; if δ is larger than the final deflection of the BPRC specimen, δ is considered to be the final deflection of the BPRC specimen; δ_{p} represents the deflection corresponding to the flexural strength of BPRC; T_{post} represents the area surrounded by the curve between the peak deflection δ_{p} and the deflection δ in the load–deflection curve of the BPRC specimen, and represents the post-peak energy values absorbed by the BPRC specimen, as displayed in Fig. 4a.

The equivalent flexural strength f_{eq1}, f_{eq2} of BPRC can be calculated as (CECS13, 2009):

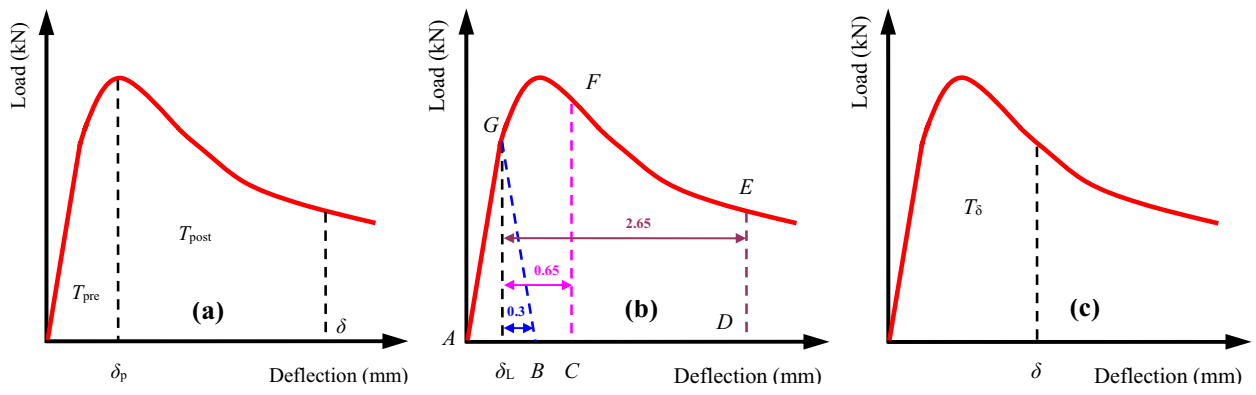

Fig. 4 Schematic calculation diagram of **a** *PCS*, **b** f_{eq1}, f_{eq2} and **c** FT_δ.

$$f_{eq1}=\frac{T_{1f}l}{0.5bh^2}, \tag{2}$$

$$f_{eq2}=\frac{T_{2f}l}{2.5bh^2}, \tag{3}$$

where T_{1f} and T_{2f} represent the contribution of the fibers to the energy absorption of concrete, where $T_{1f}=T_1-T_{cr}$; T_{cr} is the area surrounded by ABG in Fig. 4b, δ_L is the deflection of BPRC specimen corresponding to the first cracking strength; T_1 represents the area surrounded by the load–deflection curve of BPRC specimen from the coordinate origin to $\delta_L+0.65$ mm. Therefore, T_{1f} is the area surrounded by BCFG in Fig. 4b. $T_{2f}=T_2-T_{cr}$, T_2 represents the area surrounded by the load–deflection curve of the BPRC specimen from the coordinate origin to $\delta_L+2.65$ mm. Therefore, T_{2f} is the area surrounded by BDEG in Fig. 4b (CECS13, 2009). For OC, as $\delta_L+0.65$ mm and $\delta_L+2.65$ mm are higher than the maximum deflection of the specimens, the maximum deflection of both specimens is considered instead. Consequently, the tested maximum midspan deflection of BPRC specimens with fibers is 2.5 mm, so $\delta_L+2.65$ mm is assumed to be 2.5 mm for BPRC specimens with fibers.

The flexural toughness factor FT_δ of BPRC can be calculated as (Banthia et al., 2014):

$$FT_\delta=\frac{T_\delta l}{\delta bh^2}, \tag{4}$$

where δ represents the set deflection, and considered to be l/600 and l/150 herein; T_δ is the area surrounded by the load–deflection curve of the BPRC specimen from the coordinate origin to δ, as shown in Fig. 4c.

4 Analysis of Experimental Results

4.1 Compressive Strength

The change in the compressive strength of BPRC is displayed in Fig. 5a. Regardless of the matrix strength, the variation on the compressive strength of concrete is similar with the addition of BF and PF. At 0.1% content, adding single BF or PF, and hybrid BF and PF enhances the compressive strength. Adding single BF is the most effective way to enhance the compressive strength, followed by adding hybrid BF and PF, and then single PF. BF has high stiffness and is hydrophilic, which gives good compatibility and high bonding performance between BF and concrete materials (Sim et al., 2005). It is well known that the addition of fibers can reduce the shrinkage of concrete (Falliano et al., 2019). Consequently, BF not only reduces shrinkage cracks in the concrete matrix during hardening, but also inhibits crack propagation under loads, which increases the compressive strength of concrete (Branston et al., 2016). PF has low stiffness and is hydrophobic, resulting in weak bonding between PF and the matrix (Alrshoudi et al., 2020; Ranjbar et al., 2016;). Therefore, PF has a relatively lesser influence on the expansion of shrinkage cracks and load cracks of concrete, and does not substantially enhance the compressive strength. In addition, as the diameter of BF monofilaments is much smaller than that of the PF monofilaments, the number of BF monofilaments in the concrete matrix is much higher than that of PF monofilaments when the content is the same. Consequently, BF exhibits a more obvious effect on enhancing the compressive strength. According to the conclusions obtained in Refs. (Jiang et al., 2014; Ranjbar et al., 2016; Smarzewski, 2019; Smarzewski et al., 2020), BF and PF

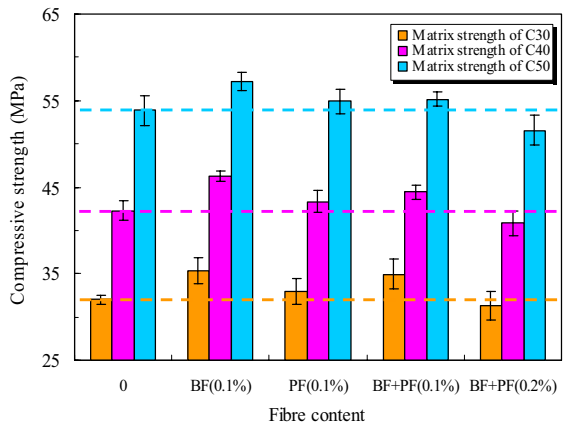

(a) Compressive strength

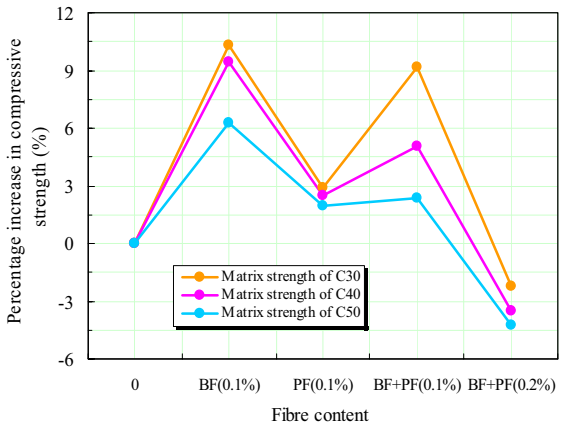

(b) Percentage increase in compressive strength

Fig. 5 Variation on the compressive strength of BPRC.

can reduce the compressive strength of concrete, which is in contrast to the results obtained herein. This discrepancy is probably due to the different matrix strength, fiber type, and fiber content. Furthermore, in this study, the addition of some mineral admixtures is not only conducive to the dispersion of fibers in the BPRC matrix, but also improves the bonding between fibers and the matrix, owing to the secondary hydration and pozzolanic effect of the mineral admixtures. This enhances the suppression effect of BF and PF on the shrinkage cracks and load cracks, and enhances the compressive strength. At the 0.1% content of hybrid BF and PF, hybrid fibers have no obvious synergistic effect, and the compressive strength of BPRC is between those of concrete with single BF and single PF. At the 0.2% content of hybrid BF and PF, the compressive strength of BPRC is smaller than that of the matrix. The poor dispersion uniformity of excess hybrid BF and PF reduces the bonding between fibers and the matrix, and increases the weak interface in concrete. In addition, more bubbles are introduced during mixing, which further reduces the compressive strength.

The variation on the growth ratio of compressive strength with the matrix strength is displayed in Fig. 5b. The enhancement effect of fibers on the compressive strength gradually decreases with the increase in the matrix strength. As a relatively small amount of fiber is used herein, a negligible effect of fibers on the compressive strength is obtained. The higher the matrix strength, the more difficult it is for fibers to enhance the compressive strength. The decreasing dispersion uniformity of excess fibers with the matrix strength increases the negative effect of fibers on the compressive strength. Therefore, the decreasing effect of 0.2% hybrid BF and PF on the compressive strength becomes more and more obvious with the matrix strength.

4.2 Flexural Load–Deflection Behavior

4.2.1 Characteristics of Flexural Load–Deflection Curve

The flexural load–deflection curve of BPRC as a function of the fiber type, fiber content, and matrix strength is displayed in Fig. 6. Adding fibers exhibits a similar influence on the flexural load–deflection curve of BPRC, regardless of the matrix strength. As shown in Fig. 7, the flexural load–deflection curve of BPRC can be roughly divided into three sections: the initial linear elastic stage (I), the deflection hardening stage (II), and the deflection softening stage (III). In general, adding BF alone increases the slope of stage I, whereas adding PF alone or hybrid BF and PF reduces the slope of stage I. The results obtained in Refs. (Bhutta et al., 2017; Li et al., 2018a) indicate that the slope of stage I is primarily affected by the concrete matrix, and is not influenced by the type and amount of fibers, which differs from the results obtained in this study. This is possibly related to the type of fibers used and the bonding between fibers and the matrix. The influence of fiber type and fiber content on the slope of stage I decreases with the matrix strength.

When the BPRC specimen reaches the first cracking strength, it enters the deflection hardening stage (II). The beginning of this stage is often accompanied by a slight decrease in the flexural load, then the flexural load quickly evolves into a nonlinear increase. As the concrete matrix has cracked at this stage, the flexural load is primarily borne by the crack bridging of the fibers. At the end of the deflection hardening stage, the BPRC specimen reaches the peak flexural strength. As shown in the inset in Fig. 6, the fiber type and fiber content exhibit a significant influence on the peak flexural strength and peak deflection (the deflection corresponding to the peak flexural strength) of the BPRC specimen. In addition, for the same fiber type and fiber content, the peak flexural strength of BPRC enhances, but the peak deflection decreases with the matrix strength.

The deflection softening stage (III) occurs after the peak flexural strength, wherein the flexural load of the BPRC specimen decreases with the increase in midspan deflection or the concrete specimens without fibers, the flexural load rapidly decreases to zero in the deflection softening stage, which indicates the significant brittle fracture characteristics. However, Adding BF and PF reduces the decreasing rate of the flexural load, indicating the ductile fracture characteristics. At the same content, the influence of PF on the ductile fracture of concrete is stronger than that of BF, but the influence of single BF and PF is weaker than that of their hybridization. The higher the hybrid fiber content, the more obvious the ductile fracture characteristics of concrete. For the same fiber type and fiber content, the reduction rate of the flexural strength of BPRC increases and the ductile fracture characteristics decrease with the matrix strength. Additionally, in the deflection softening stage, the load–deflection curve of BPRC presents some "zigzag" change, which indicates that the fibers are constantly pulled out or broken during this stage.

4.2.2 Flexural Strength

The variation on the flexural strength of BPRC with the fiber type, fiber content, and matrix strength is displayed in Fig. 8a. The flexural strength exhibits an increasing trend with the increase in matrix strength. Regardless of the matrix strength, adding BF and PF increases the flexural strength, which is in contrast to its influence on the compressive strength. At 0.1% content, BF is more conducive to increase the flexural strength of concrete than PF. This can be primarily due to the higher stiffness of BF, the larger number of monofilaments, and the

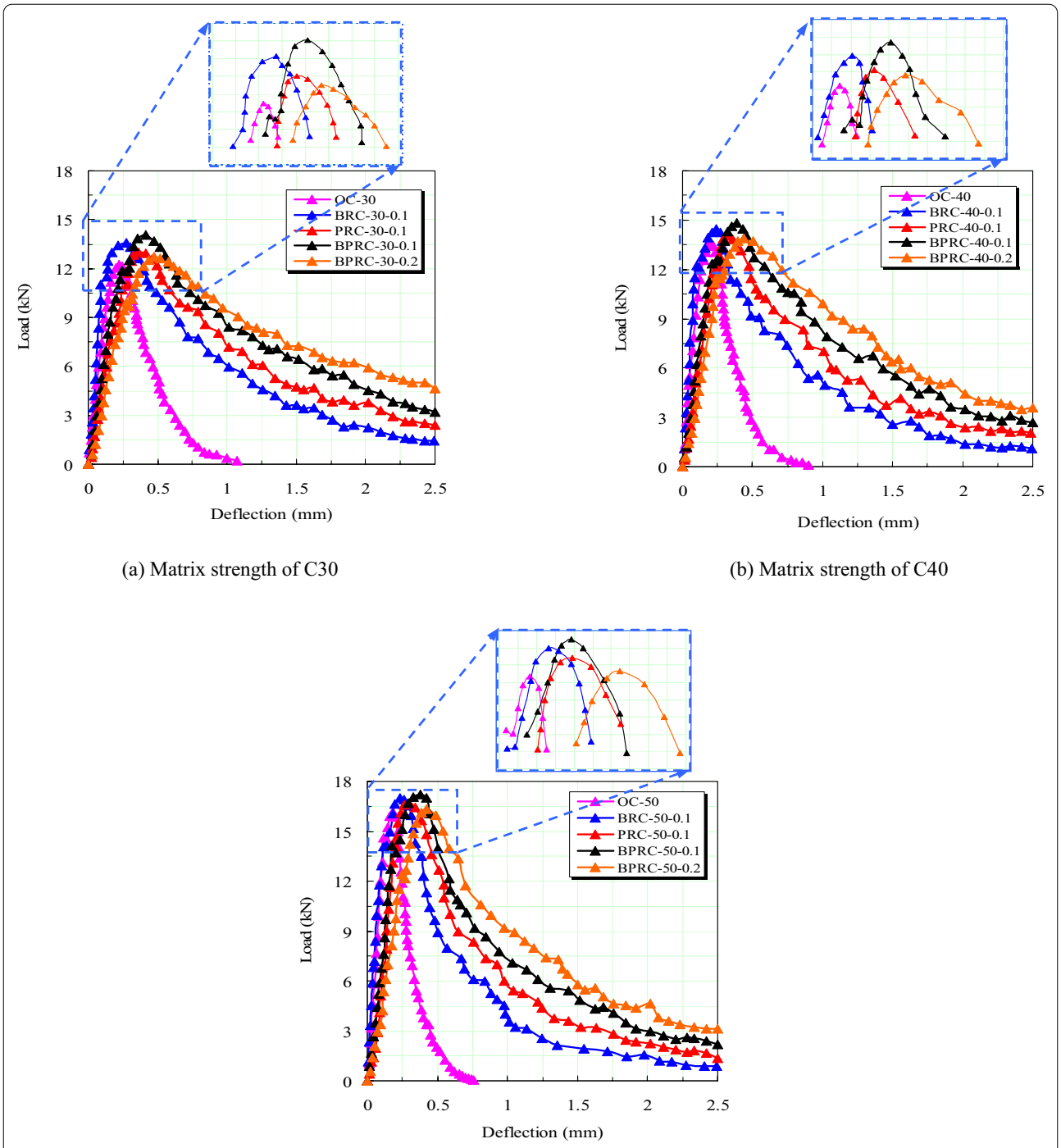

(a) Matrix strength of C30

(b) Matrix strength of C40

(c) Matrix strength of C50

Fig. 6 Load–deflection curves of BPRC.

superior bonding between BF and the matrix, which is more favorable for BF to bridge cracks. However, it is different from the increasing effect on compressive strength that hybrid BF and PF exhibits the optimal effect on increasing the flexural strength, indicating the synergistic effect of BF and PF. Due to the large size difference, hybrid BF and PF can inhibit cracks during different fracture propagation stages. For flexural fracture with single

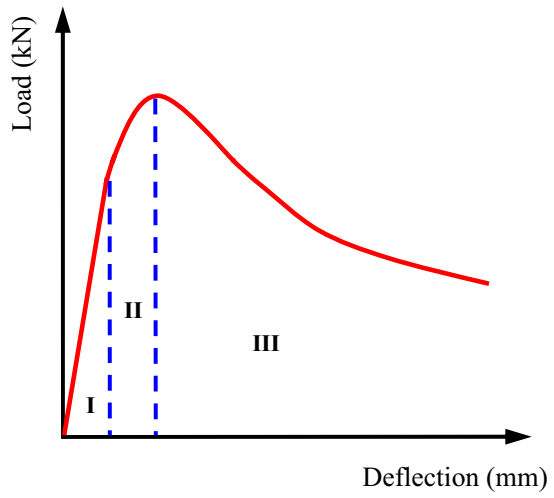

Fig. 7 Schematic pattern of load–deflection curve of BPRC.

crack, the synergistic effect of BF and PF improves the crack bridging effect to a significant extent and effectively increases the flexural strength of concrete. At a hybrid content of 0.2%, though the content of hybrid fibers is excessive, the weakening effect of fibers on the properties of the concrete matrix during single crack fracture was not evident. BF and PF, which have good bonding with concrete matrix at fracture interface, can still play an effective role in crack bridging, thereby enhancing the flexural strength. Similar to the research results of this paper, Smartzewski (2019) analyzed the influence of BF and PF on the flexural properties of high-performance concrete, and revealed that the adding single BF or PF, or hybrid BF and PF could increase the flexural strength of concrete.

The variation on the growth ratio of the flexural strength of BPRC with the matrix strength is displayed in Fig. 8b. The growth ratio of flexural strength decreases with the matrix strength, which is similar to the variation on the growth ratio of compressive strength. Thus, the increasing matrix strength weakens the influence of fibers on the flexural strength.

4.3 Flexural Fracture Morphology

The typical fracture morphology of BPRC is displayed in Fig. 9. BPRC shows the fracture morphology with a single crack. No derivative cracks are formed during the main crack propagation, but adding BF and PF exhibits a significant influence on the expansion path of the fracture crack. Without the addition of fibers, the fracture cracks are relatively straight and the brittle fracture characteristics are more evident. Adding BF and PF leads to a tortuous propagation path of fracture crack, the characteristics of ductile fracture are more obvious, and the fracture energy consumption increases (Li et al., 2018a; Yang et al., 2020). As stated by the fiber spacing theory, when the fracture crack extends to the interface between fibers and the matrix, a shear stress appears at the interface to inhibit crack expansion. This not only reduces the stress concentration at the crack tip, but also changes the crack propagation path, resulting in a "zigzag" expansion of the crack, an increase in fracture energy consumption and the flexural strength (Rossi et al., 1996). In addition, for concrete without fibers, it generally presents splitting tensile failure under the action of flexural load, and the fracture crack is relatively straight. When the fibers are

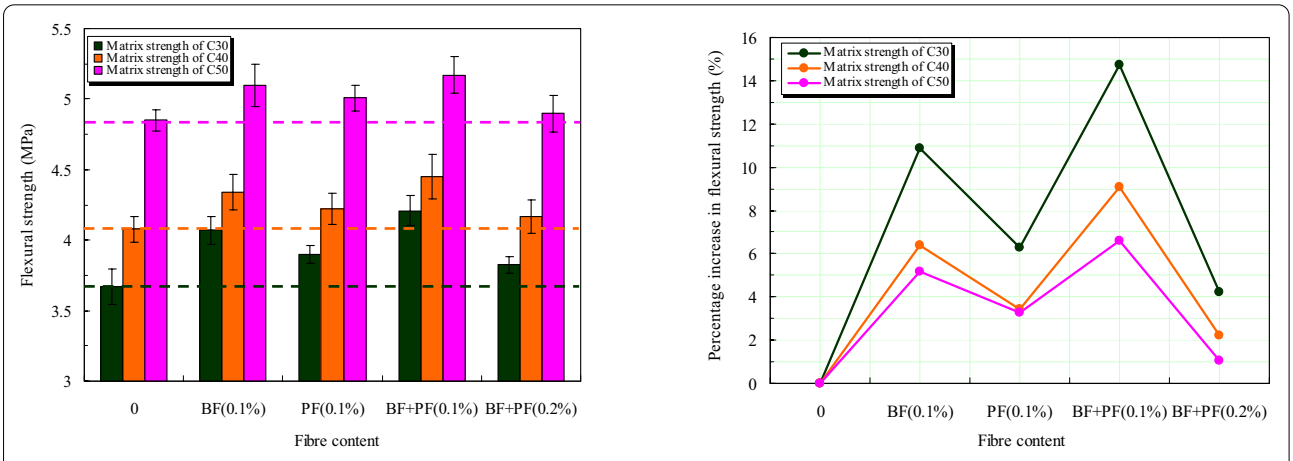

(a) Flexural strength

(b) Percentage increase in flexural strength

Fig. 8 Variation on the flexural strength with fiber content and matrix strength.

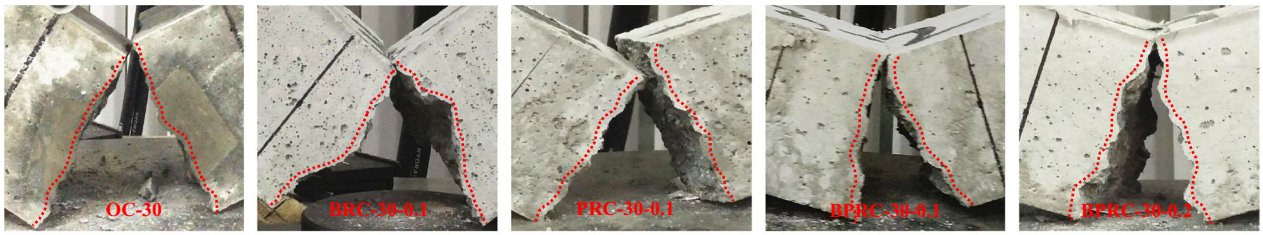

(a) Matrix strength of C30

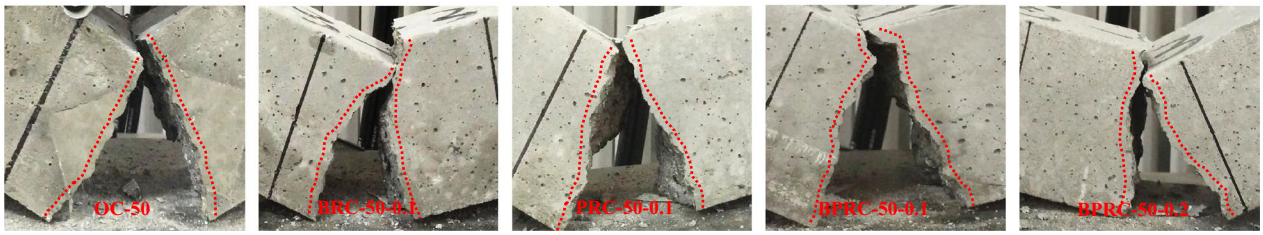

(b) Matrix strength of C50

Fig. 9 Flexural failure morphology of BPRC.

added, the fibers are gradually pulled out and the shear failure is formed after the matrix cracks. This not only increases the tortuosity of fracture cracks of concrete, but also increases the flexural strength and energy consumption of concrete (Li et al., 2018b). As displayed in Fig. 9, the tortuosity of the fracture crack in the concrete with single BF is higher than that in the concrete with single PF. The larger number of BF monofilaments leads to the higher bond performance between BF and the matrix and the more significant inhibition effect of BF on crack expansion. When hybrid BF and PF are added, the large difference in their respective sizes results in the crack bridging effect during different stages of crack expansion, which increases the tortuosity of the fracture cracks. With the hybrid fiber content, the tortuosity of the fracture cracks and the fracture energy consumption increase as well.

Through the comparison between Fig. 9a, b, it can be found that the tortuosity of the fracture cracks and the ductile fracture characteristics decrease with the matrix strength. The bonding performance between fibers and the matrix increases with the matrix strength. When the fracture crack extends to the surface of fibers, the crack propagation can lead to the fracture of fibers to a great extent owing to the high stress concentration at the crack tip. The fracture crack continues to propagate along the initial propagation direction, and the tortuosity decreases.

4.4 Failure Morphology and Action Mechanism of BF and PF

The fracture morphologies of BF and PF in concrete with matrix strengths are displayed in Fig. 10. As shown in Fig. 10a, BF has a long pull-out length, and less hydration product particles are attached to its surface at the low matrix strength. As displayed in Fig. 10b, when the matrix strength is high, BF breaks and more cement hydration product particles are attached to its surface, indicating a good bonding between BF and the matrix. As shown in Fig. 10c, d, PF exhibits a longer pull-out length than BF regardless of matrix strengths, which is primarily due to the relatively poor bonding performance between PF and the matrix. But by comparison, it is found that the pull-out length of PF decreases with the increasing matrix strength. With the matrix strength, the surface of PF shows some scratches, indicating that the increasing matrix strength enhances the friction between PF and the matrix, that is, the bonding between PF and the matrix becomes more and more significant.

As shown in Fig. 10e, f, when hybrid fibers are added, the damage morphology of BF is similar to that of BF in concrete containing single BF, but the damage

(See figure on next page.)
Fig. 10 Fracture morphologies of BF and PF in BPRC with matrix strength.

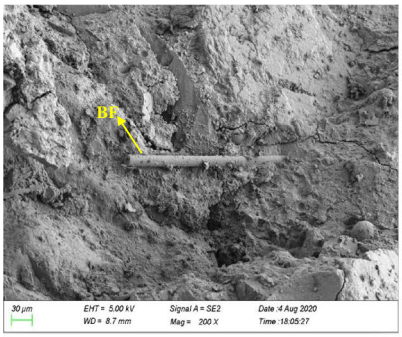

(a) BF in BRC-30-0.1

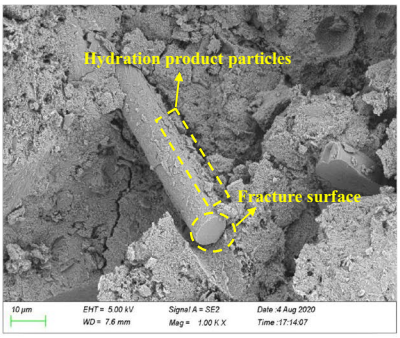

(b) BF in BRC-50-0.1

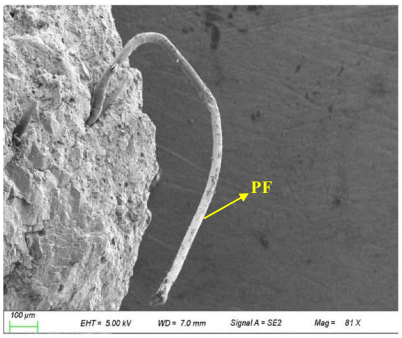

(c) PF in PRC-30-0.1

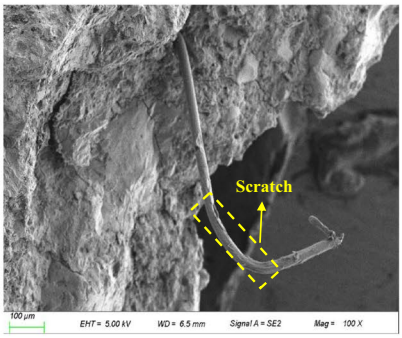

(d) PF in PRC-50-0.1

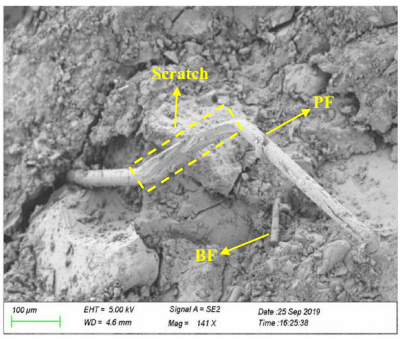

(e) BF and PF in BPRC-30-0.1

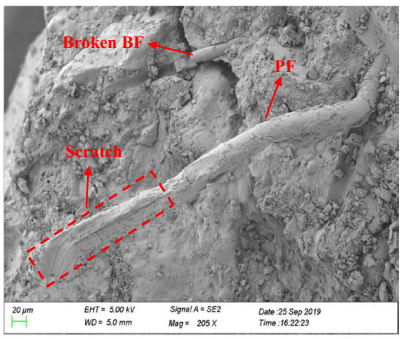

(f) BF and PF in BPRC-50-0.1

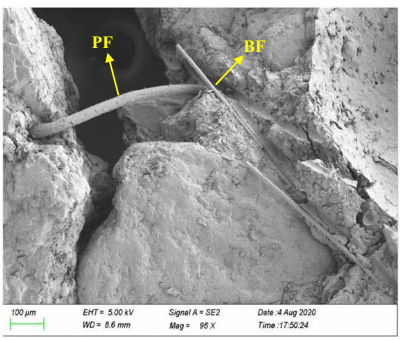

(g) BF and PF in BPRC-30-0.2

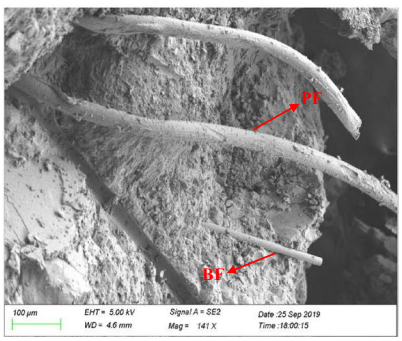

(h) BF and PF in BPRC-50-0.2

Fig. 10 (See legend on previous page.)

morphology of PF is different from that of PF in concrete containing single PF. Regardless of the matrix strength, when hybrid BF and PF are added, the surface of PF has some scratches, and the pull-out length of PF is shorter than that of PF in the concrete containing single PF. PF shows more severe surface scratches and smaller pull-out length with the matrix strength. Adding BF increases the concrete strength and inhibits the propagation of cracks around PF, that is, the restraining effect of concrete on PF and the friction between PF and the matrix also are increased to some extent, the surface damage of PF is more serious, and the pull-out length decreases.

As shown in Fig. 10g, h, at a hybrid content of 0.2%, the dispersion uniformity of BF and PF decreases. When the matrix strength is low, both BF and PF have a long pull-out length and their surfaces are smooth, which indicates that the low dispersion uniformity of fibers affects the their bonding with the matrix. As shown in Fig. 10h, when the matrix strength is high, the pull-out length of BF decreases significantly, but remains longer than that of BF in the concrete of other mix proportions. The pull-out length of PF does not change significantly, and is similar to the pull-out morphology of PF in the specimens with low matrix strength. The surface of PF does not show some scratches, indicating its low bonding with the matrix.

The fibers with different sizes can restrain the cracks at different stages of crack propagation and play a synergistic role. Generally, the fibers with small size restrain the initiation and expansion of micro-cracks, and the fibers with large size restrain the expansion of macro cracks (Yang et al., 2020). Owing to its small diameter, large number of monofilaments, and high stiffness, BF could restrain the formation, expansion of micro-cracks and the initial expansion of macro-fracture cracks. Therefore, BF is conducive to improve the flexural strength. In contrast, PF, with the large diameter, a small amount of monofilaments, and low monofilament stiffness, can inhibit the propagation of macro-fracture cracks. As shown in Fig. 11, during the initial linear elastic stage (I), the microscopic defects in the concrete remained in a stable state as they are inhibited by BF. As the flexural load increases, the BPRC specimen enters the deflection hardening stage (II), and the fracture cracks began to expand. At this time, the high stiffness and bond strength between BF and the matrix cause BF to restrict the expansion of the fracture cracks, which improves the flexural strength of concrete. As the fracture cracks continue to develop, BF is gradually broken, and the BPRC specimen enters deflection softening stage (III). During this stage, PF is gradually pulled out or stretched as the fracture cracks develop due to its low stiffness and low bond strength with the concrete matrix. Nevertheless, this reduces the propagation speed of the fracture cracks and improves the ductility and fracture toughness of concrete. Therefore, an appropriate mixing of BF and PF enhances the flexural strength and ductility of concrete.

4.5 Flexural Toughness

The variation on the fracture toughness indices of BPRC (*PCS-l*/600, *PCS-l*/150, f_{eq1}, f_{eq2}, *FT-l*/600, and *FT-l*/150) is displayed in Fig. 12. As displayed in Fig. 12a, b, at the same matrix strength, *PCS-l*/600 and *PCS-l*/150 increase with the addition of fibers, which indicates that adding fibers improves the flexural toughness of concrete. At a fiber content of 0.1%, PF exhibits a more obvious influence on *PCS-l*/600 and *PCS-l*/150 compared to BF, and the hybrid BF–PF has the most significant effect on *PCS-l*/600 and *PCS-l*/150. The *PCS-l*/600 and *PCS-l*/150 increase with the increasing hybrid fiber content. As the matrix strength increases, the *PCS-l*/600 of the concrete without fibers gradually decreases, whereas the *PCS-l*/600 of the concrete with fibers gradually increases. *PCS-l*/150 has the opposite change rule compared to *PCS-l*/600 as the matrix strength increases.

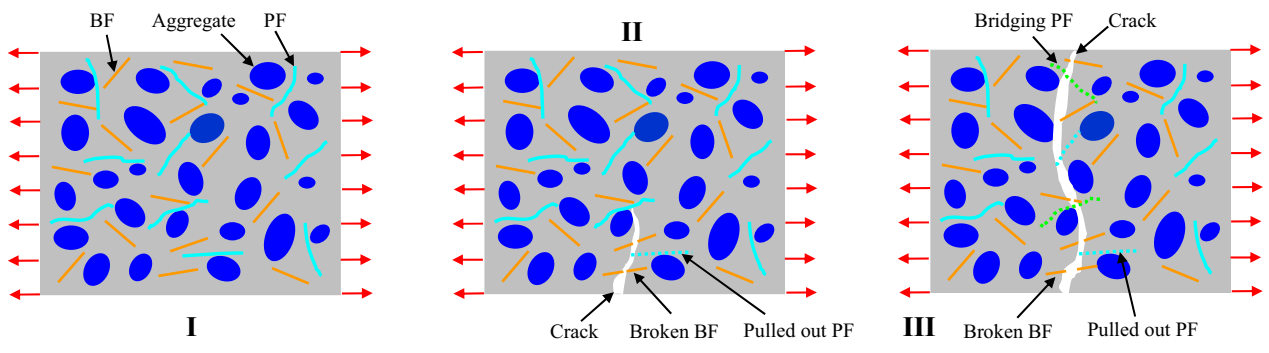

Fig. 11 Action mechanism of BF and PF.

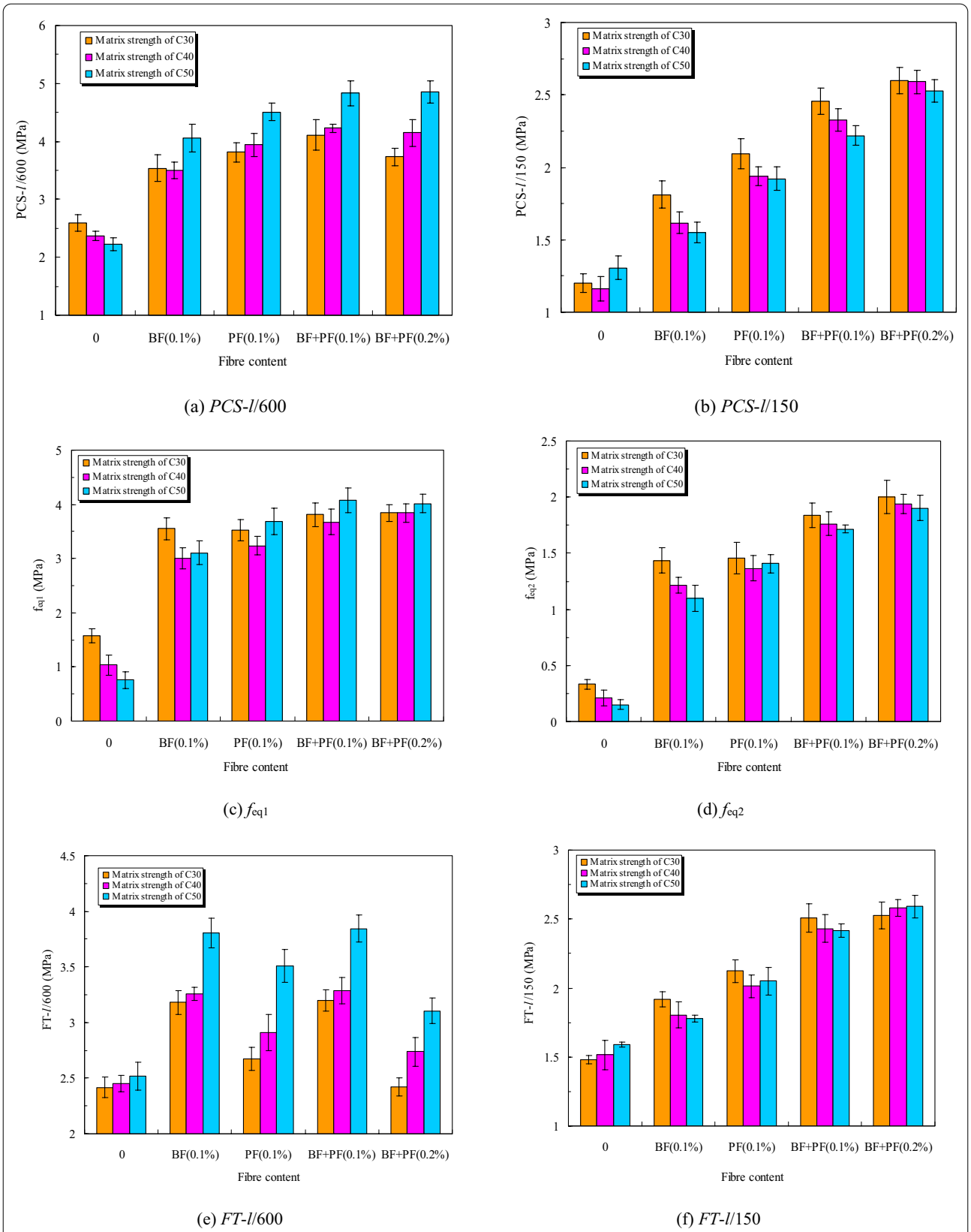

(a) *PCS-l*/600 (b) *PCS-l*/150

(c) f_{eq1} (d) f_{eq2}

(e) *FT-l*/600 (f) *FT-l*/150

Fig. 12 Variation on the flexural toughness index of BPRC.

At the same matrix strength, f_{eq1} and f_{eq2} are enhanced by adding fibers, which demonstrates that the flexural toughness of concrete increases with the addition of fibers. Fiber type and content exhibit the same influence on f_{eq1} and f_{eq2} as that on *PCS-l*/600 and *PCS-l*/150. As the matrix strength increases, the variation on f_{eq1} is more discrete, which is possibly related to the difficulty in determining the first cracking strength for f_{eq1}. However, f_{eq2} decreases with the increase in matrix strength, which indicates to some extent that a higher matrix strength leads to a more significant brittle failure of concrete.

At the same matrix strength, the variation on *FT-l*/600 is the same as that on the flexural strength with the fiber type and fiber content. *FT-l*/150 increases with the addition of fibers. At a fiber content of 0.1%, PF has a more significant improving effect on *FT-l*/150 than BF, and hybrid BF–PF has the most significant improving effect on *FT-l*/150. *FT-l*/150 increases with the increase in hybrid fiber content. *FT-l*/600 increases with the matrix strength, whereas *FT-l*/150 increases with the matrix strength for concrete without fibers and with a hybrid fiber content of 0.2%. For other proportioned concrete, *FT-l*/150 decreases with the increase in matrix strength.

When $\delta = l/600$, δ is close to the deflection corresponding to the peak flexural strength of BPRC. Therefore, the flexural toughness of BPRC is primarily affected by the flexural strength. *FT-l*/600 can better reflect the change law of the flexural toughness of BPRC than *PCS-l*/600. As stated earlier, it is difficult to determine the first cracking strength of BPRC. Therefore, f_{eq1} can not effectively characterize the flexural toughness of BPRC. When $\delta = l/150$, the fracture or pull-out of fibers increases the flexural toughness of BPRC with the same matrix strength. For concrete with different matrix strengths, because *l*/150 is much higher than the final deflection of the concrete without fibers, the flexural toughness of concrete is primarily affected by the matrix strength, and *l*/150 increases with the matrix strength. A lower matrix strength leads to a longer pull-out length of fibers, which increases the fracture energy consumption and the flexural toughness (Chen et al., 2013). At a hybrid content of 0.2%, the increase in matrix strength improves the bonding between fibers and the matrix. The fibers still show significant pull-out failure. Therefore, the higher the matrix strength is, the higher the fracture energy consumption and flexural toughness of concrete are. *FT-l*/150 is more effective in characterizing the fracture toughness of BPRC. In general, FT_δ can effectively characterize the variation on the flexural toughness of BPRC with fiber type, fiber content, and matrix strength.

Based on the definition of FT_δ and the previous analysis, *FT-l*/150 is primarily related to the influence of fibers on the ductility of concrete, whereas *FT-l*/600 is primarily related to the flexural strength of concrete. Therefore, a great (*FT-l*/150)/(*FT-l*/600) represents that the increase in the flexural toughness is due to the inhibition of fibers on the macro-fracture crack propagation. A small (*FT-l*/150)/(*FT-l*/600) represents that the increase in the flexural toughness of concrete is due to the increase in flexural strength. The variation on (*FT-l*/150)/(*FT-l*/600) is shown in Fig. 13. (*FT-l*/150)/(*FT-l*/600) of BPRC decreases with the matrix strength, indicating that a higher matrix strength results in a smaller improving effect of fibers on the ductility of concrete. The increase in the flexural toughness of concrete is primarily due to the increase in flexural strength. However, the bonding between fibers and the matrix decreases with the decrease in matrix strength, which causes the pull-out failure of fibers and increases (*FT-l*/150)/(*FT-l*/600). At the same matrix strength, according to the order of (*FT-l*/150)/(*FT-l*/600), PF is more beneficial to enhance the ductility deformation of concrete compared to BF. BF is more beneficial to enhance the strength. Although hybrid BF–PF can improve the flexural strength of concrete, it has a more significant influence on the ductility deformation of concrete, and the effect becomes more and more significant with the increasing hybrid fiber content.

5 Prediction Model for Flexural Strength of HBPRC

Based on the composite material theory, the tensile strength of fiber-reinforced composite materials can be calculated from the flexural strength of the matrix and the bonding strength between the fibers and the matrix (Han et al., 2016; Wu et al., 2018). Therefore, the tensile strength of BPRC can be calculated as:

$$\sigma_t = \sigma_{tm}(1 - V_f) + \sigma_{tf}V_f, \tag{5}$$

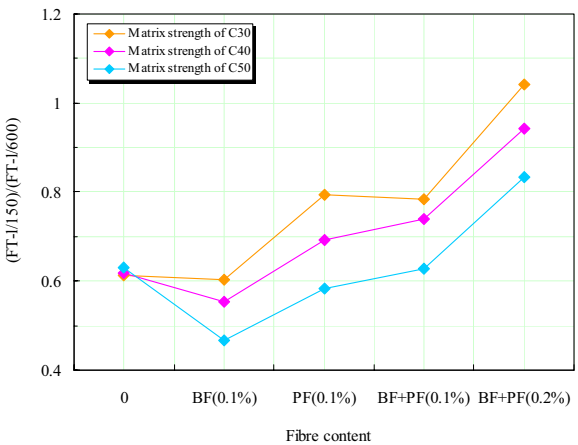

Fig. 13 Variation on (*FT-l*/150)/(*FT-l*/600) with fiber type, fiber content and matrix strength.

where σ_t, σ_{tm}, and σ_{tf} are the tensile strength of BPRC and the matrix, and the average tensile strength of fibers, respectively, and V_f is the fiber content.

As BPRC contains both BF and PF, Eq. (5) can be written as:

$$\sigma_t = \sigma_{tm}(1 - V_{f\text{-}B} - V_{f\text{-}P}) + \sigma_{tf\text{-}B}V_{f\text{-}B} + \sigma_{tf\text{-}P}V_{f\text{-}P}, \tag{6}$$

where $\sigma_{tf\text{-}B}$, $\sigma_{tf\text{-}P}$ represent the tensile strengths of BF and PF, respectively, and $V_{f\text{-}B}$, $V_{f\text{-}P}$ represents the contents of BF and PF, respectively.

The flexural and tensile strength of fiber-reinforced cementitious materials have a linear relationship (Han et al., 2016; Wu et al., 2018). Accordingly, the flexural and tensile strength of BPRC are characterized as:

$$\sigma_f = \alpha\sigma_t, \tag{7}$$

where α is the proportional coefficient between the flexural and tensile strength of BPRC. For convenience, α is approximately equal to 2.0 (Han et al., 2016).

According to Eqs. (6) and (7),

$$\begin{aligned}\sigma_f &= \alpha[\sigma_{tm}(1 - V_{f\text{-}B} - V_{f\text{-}P}) \\ &\quad + \sigma_{tf\text{-}B}V_{f\text{-}B} + \sigma_{tf\text{-}P}V_{f\text{-}P}] \\ &= \sigma_{fm}(1 - V_{f\text{-}B} - V_{f\text{-}P}) \\ &\quad + \alpha\eta_{l\text{-}B}\eta_{\theta-B}\sigma_{mtf\text{-}B}V_{f\text{-}B} \\ &\quad + \alpha\eta_{l\text{-}P}\eta_{\theta-P}\sigma_{mtf\text{-}P}V_{f\text{-}P},\end{aligned} \tag{8}$$

where σ_{fm}, $\sigma_{mtf\text{-}B}$, and $\sigma_{mtf\text{-}P}$ are the flexural strength of the matrix and the maximum flexural strengths of BF and PF, respectively; $\eta_{l\text{-}B}$, $\eta_{l\text{-}P}$ represent the length coefficients of BF and PF, respectively; $\eta_{\theta\text{-}B}$ and $\eta_{\theta\text{-}P}$ are the three-dimensional orientation coefficients of BF and PF, respectively, and are equal to 0.45 and 0.2, respectively, herein, for convenience.

The fiber length coefficients satisfy the following relationship for flexural loading (Han et al., 2016; Wu et al., 2018):

$$\eta_l = 1 - \frac{l_f^{crit}}{2l_f} \text{ when } l_f > l_f^{crit}, \tag{9}$$

$$\eta_l = \frac{l_f}{2l_f^{crit}} \text{ when } l_f \le l_f^{crit}, \tag{10}$$

where l_f and l_f^{crit} are the length and critical length of the fibers, respectively, and $l_f^{crit} = \frac{d_f\sigma_{mtf}}{2\tau}$, d_f is the diameter of the fibers, σ_{mtf} represents the maximum tensile strength of the fibers, and τ is the bonding strength between the fibers and the matrix.

When the fiber length is larger or less than the critical length, the fibers primarily exhibit a tensile or pull-out failure. According to the analysis in Sect. 4.4, BF tends to break while PF tends to pull out. Therefore, using Eqs. (9) and (10), the length coefficients of BF and PF can be calculated.

Based on Eqs. (8), (9), and (10), the flexural strength of BPRC is

$$\begin{aligned}\sigma_f &= \sigma_{fm}(1 - V_{f\text{-}B} - V_{f\text{-}P}) \\ &\quad + \alpha\eta_{\theta-B}\sigma_{mtf\text{-}B}V_{f\text{-}B} \\ &\quad - \alpha\eta_{\theta-B}V_{f\text{-}B}\frac{d_{f\text{-}B}\sigma_{mtf\text{-}B}^2}{4l_{f\text{-}B}\tau_B} \\ &\quad + \alpha\eta_{\theta-P}V_{f\text{-}P}\tau_P\frac{l_{f\text{-}P}}{d_{f\text{-}P}},\end{aligned} \tag{11}$$

where $d_{f\text{-}B}$ and $d_{f\text{-}P}$ represent the diameter of BF and PF, respectively, and $l_{f\text{-}B}$ and $l_{f\text{-}P}$ represent their lengths, respectively; and τ_B and τ_P represent the bonding strengths between BF, PF and the matrix, respectively.

Considering the physical parameters of fibers (Niu et al., 2020), τ_B and τ_P for different matrix flexural strengths can be calculated in combination with the flexural test results of BPRC as:

$$\tau_B = a_1 \ln(\sigma_{fm} + b_1), \tag{12}$$

$$\tau_P = a_2 \ln(\sigma_{fm} + b_2), \tag{13}$$

where a_1, a_2, b_1, and b_2 are the correlation coefficients, whose values are 0.35298, 0.30734, 14.07226, and 8.79039, respectively.

The flexural strength prediction model for BPRC is proposed by combining Eqs. (11)–(13). Fig. 14 displays the comparison between the results calculated using the prediction model and the experimental results. The predicted flexural strength of the model established herein is consistent with the flexural strength of BPRC

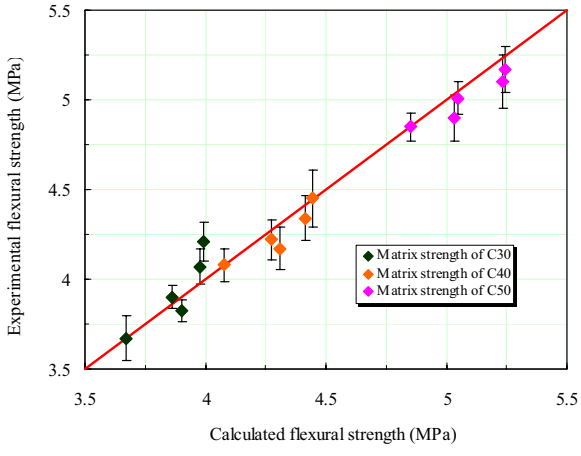

Fig. 14 Predicted and experimental values of flexural strength of BPRC.

obtained experimentally, which demonstrates the validity of the proposed flexural strength prediction model for BPRC. However, the relevant parameters (α, $\eta_{\theta\text{-B}}$, $\eta_{\theta\text{-P}}$) are empirical values that are based on the research results of fiber-reinforced cement-based composites, and are used to ensure the calculation convenience. To further improve the theoretical basis and effectiveness of the proposed prediction model, the systematic experimental research must be carried out to determine accurate parameters of BPRC.

6 Conclusions

The flexural properties of BPRC with different matrix strengths were systematically investigated. The change rules of the load–deflection curve, flexural strength, fracture morphology, fiber failure morphology, and flexural toughness of BPRC were analyzed, and a prediction model for the flexural strength of BPRC was established. The main conclusions are drawn as follows:

1. When the content of fibers is 0.1%, the addition of fibers can improve the compressive strength of concrete, and a BF content of 0.1% has the most obvious effect on improving the compressive strength. However, with the increase of the matrix strength, the improving proportion of fibers to compressive strength decreases gradually. A hybrid fiber content of 0.2% exhibits a negative effect on the compressive strength of concrete.
2. The load–deflection curve of BPRC contains the initial linear elastic stage, deflection hardening stage, and deflection softening stage. Adding BF and PF enhances the ductility of concrete, and hybrid BF–PF exhibits a most significant enhancing effect. The ductility deformation of BPRC decreases with the increasing matrix strength.
3. Adding BF and PF enhances the flexural strength of concrete. A hybrid fiber content of 0.1% exhibits the most significant improving effect on the flexural strength. A higher matrix strength leads to a smaller improving effect of fibers on the flexural strength of concrete.
4. BPRC has a fracture morphology with single crack. Adding BF and PF increases the tortuosity of the fracture cracks. The addition of hybrid fibers significantly increases the tortuosity of the fracture cracks and the energy consumption of concrete. The tortuosity of the fracture cracks decreases with the increase in matrix strength.
5. As the matrix strength increases, the damage of fibers is aggravated. With hybrid BF–PF, the failure morphology of BF does not change significantly, but the surface damage of PF is aggravated. At an excessive hybrid fiber content, both BF and PF exhibits a longer pull-out length and the damage morphology of PF does not change significantly with the increase in matrix strength, whereas the pull-out length of BF decreases.
6. FT_{δ} can effectively characterize the variation on the flexural toughness of BPRC with fiber type, fiber content, and matrix strength. *FT-l*/600 is primarily related to the matrix strength, and a hybrid fiber content of 0.1% exhibits the most significant improving effect on *FT-l*/600. *FT-l*/150 is primarily related to the influence of the failure morphology of fibers on the fracture energy consumption of concrete, and a hybrid fiber content of 0.2% is most beneficial to improve *FT-l*/150. An analysis of the results indicates that BF is more beneficial to enhance the strength of concrete, whereas PF is more beneficial to enhance ductility deformation of concrete.
7. According to the composite material theory, a flexural strength prediction model for BPRC is established based on the matrix strength, fiber length, fiber diameter, fiber content, and tensile strength, and the predicted results well agree with the experimental ones, indicating the validity of the proposed model.

Acknowledgements
The authors gratefully acknowledge the financial support of the National Natural Science Foundation of China (51608432, 51878549).

Author contributions
All authors contributed substantially to all aspects of this article. All authors read and approved the final manuscript.

Authors' information
Qiang Fu is an Associate Professor at Xi'an University of Architecture and Technology, Shaanxi, Xi'an, 710055, China.
Zhaorui Zhang is a MS student at Xi'an University of Architecture and Technology, Shaanxi, Xi'an, 710055, China.
Wenrui Xu is a MS student at Xi'an University of Architecture and Technology, Shaanxi, Xi'an, 710055, China.
Xu Zhao is a MS student at Xi'an University of Architecture and Technology, Shaanxi, Xi'an, 710055, China.
Lu Zhang is a PhD student at Xi'an University of Architecture and Technology, Shaanxi, Xi'an, 710055 China.
Yan Wang is an Associate Professor at Xi'an University of Architecture and Technology, Shaanxi, Xi'an, 710055, China.
Ditao Niu is a Professor at Xi'an University of Architecture and Technology, Shaanxi, Xi'an, 710055, China.

Funding
This study was funded by the National Natural Science Foundation of China (Grant No. 51590914, 51608432).

Availability of data and materials
All data used during the study appear in the submitted article.

Declarations

Competing interests
The authors declare that they have no conflict of interest.

Author details
[1]School of Civil Engineering, Xi'an University of Architecture and Technology, Xi'an 710055, People's Republic of China. [2]State Key Laboratory of Green Building in Western China, Xi'an University of Architecture and Technology, Xi'an 710055, People's Republic of China. [3]College of Materials Science and Engineering, Xi'an University of Architecture and Technology, Xi'an 710055, People's Republic of China.

Received: 23 December 2021 Accepted: 4 April 2022
Published online: 23 June 2022

References

Alrshoudi, F., et al. (2020). Drying shrinkage and creep properties of prepacked aggregate concrete reinforced with waste polypropylene fibers. *Journal of Building Engineering, 26*, 101522.
Banthia, N., et al. (2007). Toughness enhancement in steel fiber reinforced concrete through fiber hybridization. *Cement and Concrete Research, 37*(9), 1366–1372.
Banthia, N., et al. (2014). Fiber synergy in hybrid fiber reinforced concrete (HyFRC) in flexure and direct shear. *Cement and Concrete Composites, 48*, 91–97.
Bhutta, A., et al. (2017). Flexural behaviors of geopolymer composites reinforced with steel and polypropylene macro fibers. *Cement and Concrete Composites, 80*, 31–40.
Branston, J., et al. (2016). Influence of basalt fibres on free and restrained plastic shrinkage. *Cement and Concrete Composites, 74*, 182–190.
CECS 13. (2009). Standard test methods for fiber reinforced concrete. *China Construction Engineering Association*, China.
Chen, Z., et al. (2013). Quasi-static and dynamic compressive mechanical properties of engineered cementitious composite incorporating ground granulated blast furnace slag. *Materials and Design, 44*, 500–508.
Dilbas, H., et al. (2020). Influence of basalt fiber on physical and mechanical properties of treated recycled aggregate concrete. *Construction and Building Materials, 254*, 119216.
Domenico, D. D., et al. (2020). Bond behavior and ultimate capacity of notched concrete beams with externally-bonded FRP and PBO-FRCM systems under different environmental conditions. *Construction and Building Materials, 265*, 121208.
Dong, J., et al. (2008). Comparative flexural behavior of four fiber reinforced cementitious composites. *Cement and Concrete Composites, 30*(10), 917–928.
Dong, S., et al. (2019). Flexural toughness and calculation model of super-fine stainless wire reinforced reactive powder concrete. *Cement and Concrete Composites, 104*, 103367.
Falliano, D., et al. (2019). Compressive and flexural strength of fiber-reinforced foamed concrete: Effect of fiber content, curing conditions and dry density. *Construction and Building Materials, 198*, 479–493.
Fu, Q., et al. (2018). Impact response of concrete reinforced with hybrid basalt-polypropylene fibers. *Powder Technology, 326*, 411–424.
GB/T50081–2002. (2002). Standard for test method of mechanical properties on ordinary concrete. *China Building Materials Academy*, China.
GB/T50080–2016. (2016). Standard for test method of performance on ordinary fresh concrete. *China Academy of Building Sciences*, China.
Han, B., et al. (2016). Microstructure related mechanical behaviors of short-cut super-fine stainless wire reinforced reactive powder concrete. *Materials and Design, 96*, 16–26.
He, B., et al. (2020). Effects of fibers on flexural strength of ultra-high-performance concrete subjected to cryogenic attack. *Construction and Building Materials, 265*, 120323.
Jiang, C., et al. (2014). Experimental study on the mechanical properties and microstructure of chopped basalt fibre reinforced concrete. *Materials and Design, 58*, 187–193.
Li, B., et al. (2018a). Experimental investigation on the flexural behavior of steel-polypropylene hybrid fiber reinforced concrete. *Construction and Building Materials, 191*, 80–94.
Li, B., et al. (2018b). Effects of fiber type, volume fraction and aspect ratio on the flexural and acoustic emission behaviors of steel fiber reinforced concrete. *Construction and Building Materials, 181*, 474–486.
Marcos-Meson, V., et al. (2018). Corrosion resistance of steel fibre reinforced concrete—A literature review. *Cement and Concrete Research, 103*, 1–20.
Mastali, M., et al. (2018). Characterization and optimization of hardened properties of self-consolidating concrete incorporating recycled steel, industrial steel, polypropylene and hybrid fibers. *Composites, Part b: Engineering, 151*, 186–200.
Niu, D., et al. (2020). A 3D-IFU model for characterising the pore structures of hybrid fibre-reinforced concrete. *Materials and Design, 188*, 108473.
Ralegaonkar, R., et al. (2018). Application of chopped basalt fibers in reinforced mortar: A review. *Construction and Building Materials, 164*, 589–602.
Ranjbar, N., et al. (2016). Mechanisms of interfacial bond in steel and polypropylene fiber reinforced geopolymer composites. *Composites Science and Technology, 122*, 73–81.
Rossi, P., et al. (1996). Effect of loading rate on the tensile behaviour of concrete: Description of the physical mechanisms. *Materials and Structures, 29*, 116–118.
Rybin, V., et al. (2013). Alkali resistance, microstructural and mechanical performance of zirconia-coated basalt fibers. *Cement and Concrete Research, 53*, 1–8.
Shi, F., et al. (2020). Post-cracking behaviour of basalt and macro polypropylene hybrid fibre reinforced concrete with different compressive strengths. *Construction and Building Materials, 262*, 120108.
Sim, J., et al. (2005). Characteristics of basalt fiber as a strengthening material for concrete structures. *Composites, Part b: Engineering, 36*(6–7), 504–551.
Smarzewski, P. (2019). Influence of basalt-polypropylene fibres on fracture properties of high performance concrete. *Composite Structures, 209*, 23–33.
Smarzewski, P. (2020). Flexural toughness evaluation of basalt fibre reinforced HPC beams with and without initial notch. *Composite Structures, 235*, 111769.
Sukontasukkul, P., et al. (2018). Flexural performance and toughness of hybrid steel and polypropylene fibre reinforced geopolymer. *Construction and Building Materials, 161*, 37–44.
Sun, X., et al. (2019). Mechanical properties tests and multiscale numerical simulations for basalt fiber reinforced concrete. *Construction and Building Materials, 202*, 58–72.
Uygunoglu, T. (2008). Investigation of microstructure and flexural behavior of steel-fiber reinforced concrete. *Materials and Structures, 41*, 1441–1449.
Walton, P., et al. (1975). Cement-based composites with mixtures of different types of fibres. *Composites, 6*(5), 209–216.
Wang, D., et al. (2019). Mechanical properties of high performance concrete reinforced with basalt fiber and polypropylene fiber. *Construction and Building Materials, 197*, 464–473.
Wang, J., et al. (2012). Effect of shrinkage reducing admixture on flexural behaviors of fiber reinforced cementitious composites. *Cement and Concrete Composites, 34*, 443–450.
Wu, F., et al. (2020). Compressive and flexural properties of ultra-high performance fiber-reinforced cementitious composite: The effect of coarse aggregate. *Composite Structures, 236*, 111810.
Wu, Z., et al. (2018). How do fiber shape and matrix composition affect fiber pullout behavior and flexural properties of UHPC ? *Cement and Concrete Composites, 90*, 193–201.
Yang, Y., et al. (2020). Reinforcement effects of multi-scale hybrid fiber on flexural and fracture behaviors of ultra-low-weight foamed cement-based composites. *Cement and Concrete Composites, 108*, 103509.
Yap, S., et al. (2014). Flexural toughness characteristics of steel-polypropylene hybrid fibre-reinforced oil palm shell concrete. *Materials & Design, 57*, 652–659.
Yoo, D., et al. (2013). Effect of shrinkage reducing admixture on tensile and flexural behaviors of UHPFRC considering fiber distribution characteristics. *Cement and Concrete Research, 54*, 180–190.
Zhang, H., et al. (2019). Research on the impact response and model of hybrid basalt-macro synthetic polypropylene fiber reinforced concrete. *Construction and Building Materials, 204*, 303–316.
Zhong, H., et al. (2020). Experimental study on engineering properties of concrete reinforced with hybrid recycled tyre steel and polypropylene fibres. *Journal of Cleaner Production, 259*, 120914.

Publisher's Note